Tr. J. of Chemistry
20 (1996) , 9 – 26.

Analysis of Retention in Supercritical Fluid Chromatography and its Relation to Solubility

Z. Sermin GÖNENÇ, Uğur AKMAN
Department of Chemical Engineering,
Boğaziçi University,
80815 Bebek, Istanbul-TURKEY

Aydın K. SUNOL*
Department of Chemical Engineering,
University of South Florida,
Tampa, FL 33620

Received 20.9.1994

The effects of temperature, pressure and supercritical fluid density on the solubility-retention relationship of solutes in supercritical fluid chromatography are investigated. New retention data for naphthalene, phenanthrene, benzoic acid and 2-methoxy-naphthalene is obtained as a function of pressure at different temperatures. The bulk of the data is taken near the critical region of the mobile gas where the anomalities are expected. This data is used to compare two approaches for thermodynamic modeling of pressure dependence of solute retention. In these approaches, mobile-phase partial molar volumes of the solutes are determined either from bulk solubility data or from infinite-dilution fugacity coefficients. In both approaches, an integrated from of retention pressure relation is utilized to explicitly reveal the nature of interactions between the stationary phase and the solute. The approach that utilizes infinite-dilution fugacity coefficient better predicts the pressure dependence of retention, especially for solutes that are substantially soluble near the critical point of the mobile phase. Relationships between pressure and temperature dependence of solubility and retention of solutes are also investigated.

Introduction

Supercritical Fluid Chromatography (SFC) is a rather recent tool that continues to receive considerable attention for chemical analysis and thermophysical property estimation. Given the existing difficulties in thermophysical property measurement and estimation under supercritical conditions, any SFC based approach deserves a special attention, in part due to its promise in high data turnaround. Although the area is quite new, there is some foundation, from similar GC and HPLC work, to build upon. The retention of a solute in the chromatographic column in SFC is dependent on the strength of sorption of the solute on

* To whom correspondence should be addressed.

(and within) the stationary phase, as well as the solubility of the solute in the supercritical mobile phase. Since many thermophysical properties can be related to the retention in SFC, a thorough investigation of the characteristics of retention including its relation to solubility in SFC is essential.

The capacity ratio, k, of the component under test is given by

$$k = \frac{c_s}{c_m}\frac{V_{ts}}{V_{tm}} = \frac{y_s}{y_m}\frac{V_m}{V_s}\frac{V_{ts}}{V_{tm}}, \tag{1}$$

where c_s and c_m are concentrations of the solute in the stationary and mobile phases, V_{ts} and V_{tm} are the total volumes of the stationary and mobile phases; y_s and y_m are mole fractions of the solute in the stationary phase and the mobile phase; and V_s and V_m are molar volumes of the stationary phase the mobile phase.

The capacity ratio, k, can be determined relatively easily and accurately from SFC experiments since, in linear chromatography, it is related to the total retention time, t, of the solute and to the retention time of an inert substance, t_0, according to:

$$k = \frac{(t - t_0)}{t_0}. \tag{2}$$

Equating the chemical potentials of solute in the mobile and stationary phases, one can obtain the change in the chromatographic retention of a solute with pressure (Van Wasen and Schneider[1] and Yonker and co-workers[2]) as

$$\left[\frac{\partial lnk}{\partial P}\right]_T = \frac{1}{RT}[\bar{V}_m^{\infty} - \bar{V}_s^{\infty}] - \left[\frac{\partial ln\rho_m}{\partial P}\right]_T + \left[\frac{\partial ln\rho_s}{\partial P}\right]_T + \left[\frac{\partial ln(V_{ts} - V_{tm})}{\partial P}\right]_T, \tag{3}$$

where $\bar{V}_m^{\infty}$ and $\bar{V}_s^{\infty}$ are the partial molar volumes of the solute in the mobile phase and stationary phase at infinite dilution; and ρ_m and ρ_s are molar densities of the mobile and stationary phases. If the stationary phase is incompressible, Equation 3 reduces to:

$$\left[\frac{\partial lny_m}{\partial P}\right]_T = \frac{1}{RT}[\bar{V}_m^{\infty} - \bar{V}_s^{\infty}] - \kappa_m, \tag{4}$$

where κ_m is the isothermal compressibility of the mobile phase. The solubility of a solute in a supercritical fluid at infinite dilution is given by Gitterman and Prococcia[3] as

$$\left[\frac{\partial lny_m}{\partial P}\right]_T = \frac{1}{RT}[V_{sol} - \bar{V}_m^{\infty}], \tag{5}$$

where V_{sol} is the molar volume of the solid solute. In the above equation, it is assumed that the solute's infinite-dilution partial molar volume, $\bar{V}_m^{\infty}$, is approximately equal to that of a saturated solution, $\bar{V}_m$. This assumption is valid for small amounts of solute in the mobile phase.

Yonker et al.[2] and Bartle et al.[4,5] further exploit the low solute solubilities in the mobile phase and use bulk solubility data to calculate $\bar{V}_m^{\infty}$ from Equation 5 since solid solubilities in supercritical carbon dioxide are low.

Substituting the explicit form of $\bar{V}_m^{\infty}$ from Equation 5 into Equation 4 gives:

$$\left[\frac{\partial lnk}{\partial P}\right]_T = \frac{1}{RT}[V_{sol} - \bar{V}_s^{\infty}]\left[\frac{\partial lny_m}{\partial P}\right]_T - \kappa_m, \tag{6}$$

Through Equation 6, Yonker et al.[2] calculated constant values of the partial molar volumes of the solutes in the stationary phase for given stationary phase and different film thicknesses. The authors reported

values of $\bar{V}_s^{\infty}$ which are positive and close to the molar solid volume of the solute. However, these data show differences in $\bar{V}_s^{\infty}$ values for different stationary phases. This difference was attributed to the possible effect of stationary phase interactions between the bonded polymeric phase and the solute. They also reported differences in $\bar{V}_s^{\infty}$ values for different film thicknesses for the same stationary-phase material. As the stationary-phase film thickness increased, $\bar{V}_s^{\infty}$ decreased. This effect was explained by the liquid-like behavior of the stationary phase with increasing film thickness which made the polymer more able to solvate the solute[6]. Yonker and Smith[7] also reported negative $\bar{V}_s^{\infty}$ values for naphthalene at 308 K. Yonker and Smith[8] distinguish between three cases where $\bar{V}_s^{\infty}$ is either equal to or less or greater than the molar volume of the solute. The first case corresponds to zero intermolecular interaction between the stationary phase and the solute. In the second and third cases, the solute partitions between the solute and the stationary phase. When $\bar{V}_s^{\infty}$ was assumed to vary linearly with pressure, the retention of naphthalene could be extrapolated accurately up to 40 MPa at 308 K.

Bartle et al.[4,5] extended the data base to more solutes while comparing solubility-retention relationship in HPLC and SFC. When the stationary phase did not swell, the solute/stationary-phase interactions were suggested to be independent of the mobile phase. For such a system, through judious selection of a stationary phase, $\bar{V}_s^{\infty}$ can be equated to the molar volume of the solid solute. This results in a linear relationship between retention k and reciprocal of the solubility $(1/y_m\rho_m)$.

In the present study, two approaches, both using an integrated form of the pressure-retention relationship, are compared for modeling the pressure dependence of the partial molar volume of the solute in the stationary phase. In the first approach, the partial molar volume of the solute in the mobile phase is calculated using bulk solubility data. In the second approach, the partial molar volume of the solute in the mobile phase is calculated using infinite-dilution fugacity coefficient. The literature data for retention-pressure and corresponding analysis lacks due weighing of the anomalities near the critical region. Therefore, several solutes were used, at different temperatures, to study pressure dependence of $\bar{V}_s^{\infty}$, particularly near the critical point of the mobile phase. Two approaches are compared to explore how they differ in determining $\bar{V}_s^{\infty}$. Also, retention data were taken for a solute (2-methoxy-naphthalene) for which there is no bulk solubility data available. The partial molar volume of this solute in the stationary phase was estimated using the second approach. The numerical problems associated with differential data were alleviated through working with an integrated form of the pressure-retention relationship.

Experimental

The experiments were carried out on a Lee Scientific supercritical fluid chromatograph Series 600. The chromatograph was fitted with a five meter long, 100 μm ID capillary column coated with poly-dimethylsiloxane of 0.25 μm film thickness. The detections were made with the aid of a flame ionization detector. Column temperature and mobile-phase pressure were controlled to an accuracy of $\pm$ 0.1 K and $\pm$ 0.01 MPa, respectively. Retention times were measured using the computer system of the chromatograph with an accuracy of 0.02 seconds. Carbon dioxide was used as the carrier fluid. The samples (dissolved in n-pentane) were introduced into the column by means of an automatic injection system. The samples were at infinite dilution in n-pentane. Methane was used as the inert material to determine the retention time of a compound which is sorbed negligibly (if at all) on the column material. Retention data were taken for naphthalene, phenanthrene, benzoic acid and 2-methoxy-naphtalene at various pressures and at isothermal conditions (Table 1). Some details of the experiments can also be found in Ref. 9.

Table 1. Temperature and Pressure Ranges of Experimental Retention Data.

Solute	Temperature [K]	Pressure [MPa]
Naphthalene	313	6.08-9.63
Naphthalene	318	6.08-1013
Naphthalene	323	6.08-10.64
Phenanthrene	313	9.32-11.15
Phenanthrene	323	9.63-11.65
Benzoic Acid	313	8.41-9.93
Benzoic Acid	323	8.61-10.64
2-Methoxy-Naphthalene	313	8.10-9.93
2-Methoxy-Naphthalene	323	8.10-11.15

Theory and Method

In order to calculate the partial molar volume of the solute in the stationary phase, $\bar{V}_s^{\infty}$ from Equation 4, the infinite-dilution partial molar volume of solute in the supercritical mobile-phase, $\bar{V}_m^{\infty}$ has to be evaluated. $\bar{V}_m^{\infty}$ can be calculated either from infinite-dilution supercritical-phase solubility data or from an equation of state. The parameters of the equation of state can be obtained from supercritical solvent/solute solubility data. Although the former is the desired method, lack of extensive infinite-dilution density data bars this option. Therefore, one may follow two different approaches in calculating $\bar{V}_m^{\infty}$.

In Approach A, $\bar{V}_m^{\infty}$ is substituted into Equation 4 from Equation 5, and the resulting equation is:

$$d\ln(k\rho_m y_m) = \frac{1}{RT}(V_{sol} - \bar{V}_s^{\infty})dP. \tag{7}$$

If $\bar{V}_s^{\infty}$ is independent of pressure, the integrated form of Equation[7] would give a straight line and $\bar{V}_s^{\infty}$ can then the be calculated from the slope.

Since equilibrium solubilities of some solutes of interest (e.g. naphthalene) are too high to be considered at infinite dilution, the use of the equilibrium mole fractions in calculating $\bar{V}_m^{\infty}$ may not be very desirable. Therefore, in Approach B, $\bar{V}_m^{\infty}$ was calculated from the following relation[8]:

$$\left[\frac{\partial \ln \hat{\phi}_m}{\partial P}\right]_T = \frac{\bar{V}_m}{RT} - \frac{1}{P}, \tag{8}$$

where $\hat{\phi}_m$ is the figacity coefficient of the solute in the mobile phase. This approach avoids the use of the assumption that the solute's partial molar volume at infinite dilution approximates that of a saturated solution. Solving $\bar{V}_m$ at infinite dilution of the solute from Equation 8 gives:

$$\bar{V}_m^{\infty} = RT\left[\frac{1}{P} + \lim_{y\to 0}\left[\frac{\partial \ln \hat{\phi}_m}{\partial P}\right]_T\right] = RT\left[\frac{1}{P} + \left[\frac{\partial \ln \hat{\phi}_m^{\infty}}{\partial P}\right]_T\right], \tag{9}$$

where $\hat{\phi}_m^{\infty}$ is the fugacity coefficient of the solute in the mobile phase at infinite dilution. Substituting Equation 9 into Equation 4 results in:

$$d\ln\frac{k\rho_m}{\hat{\phi}_m^{\infty}P} = -(\bar{V}_s^{\infty}/RT)dP. \tag{10}$$

Assuming that $\bar{V}_s^{\infty}$ is constant, Equation 10 can be integrated to obtain a linear relation and $\bar{V}_s^{\infty}$ can be extracted from the slope of the linear equation using retention-pressure data. The procedures used in approaches A and B to calculate $\bar{V}_s^{\infty}$ are shown in Figure 1a and 1b.

Solubility data of the solutes of interest in carbon dioxide were obtained from literature. Table 2 gives the sources[10,11,12,13,14] and ranges of bulk solubility data used in the calculations.

Table 2. Solubility Data

Solute	Temperature [K]	Pressure [MPa]	Reference
Naphthalene	308-338	8.7-29.1	(10)
Phenanthrene	308	10.0-35.0	(11)
Phenanthrene	318-338	12.0-28.0	(12)
Benzoic Acid	308	12.0-28.0	(13)
Benzoic Acid	318-338	12.0-28.0	(12)

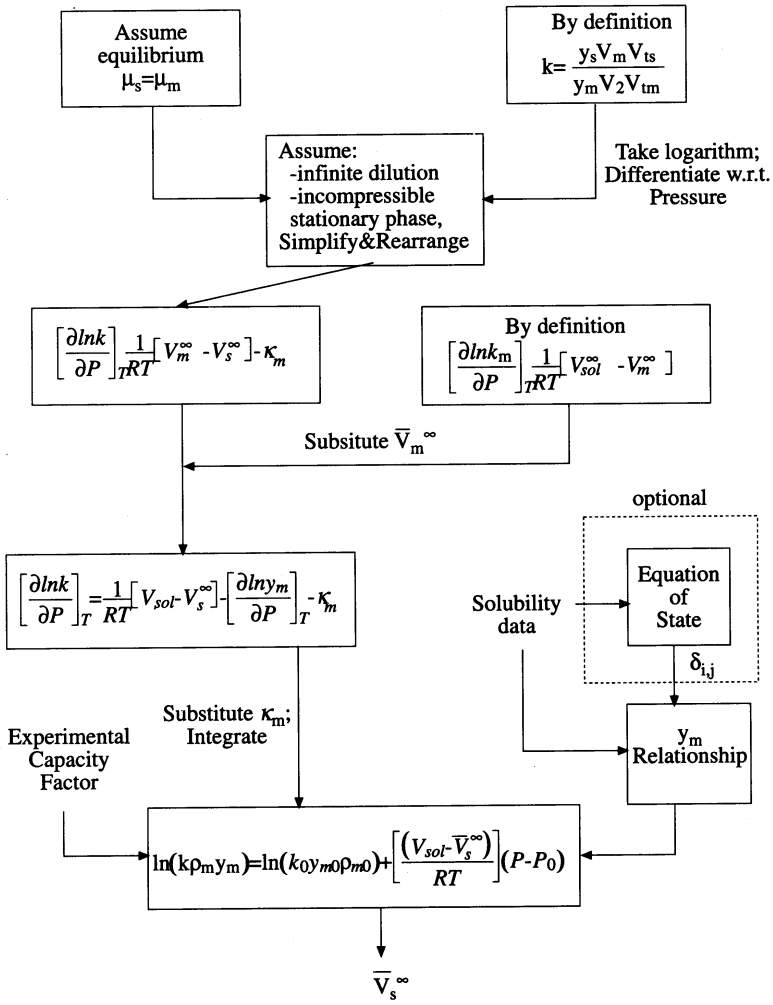

Figure 1a. Procedure for calculation of $\bar{V}_s^{\infty}$ using solubility data.

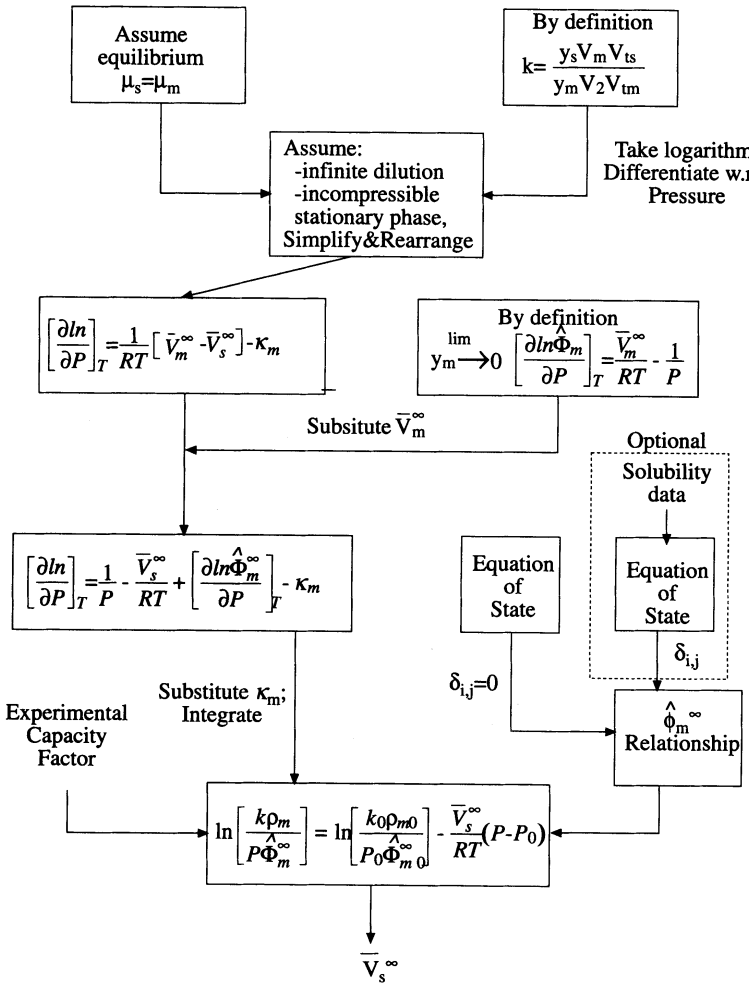

Figure1b. Procedure for calculation of $\bar{V}_s^{\infty}$ using infinnite-dilution fugacity coefficient

The Peng-Robingson Equation Of State (PRXEOS)[15] is often used for representation of solubility data. For the binary systems of interest, it is advantageous to use the mixing rule (Equation 11) of Panagiotopoulos and Reid[16] which was developed for asymmetric polar systems:

$$a_{mix}=\sum_i\sum_j y_i y_j\sqrt{a_i a_j}[1-\delta_{ij}+(\delta_{ij}-\delta_{ji})y_i], \tag{11}$$

where δ_{ij} and δ_{ji} are the binary interaction parameters. If $\delta_{ij}=\delta_{ji}$, Equation (11) reduces to the conventional combining rule.

Van der Waals one-fluid model was used to obtain the mixture parameters. The pure component parameters for the solutes and for the supercritical carbon dioxide were obtained from the usual acentric-factor correlation.

The solid-vapor equilibrium is described with the following thermodynamic relation:

$$y=\frac{P_{sub}(T)}{P\hat{\phi}_m(T,P,y)}\exp\left[\frac{V_{sol}(P-P_{sub}(T))}{RT}\right] \tag{12}$$

where $P_{sub}(T)$ is the temperature-dependent sublimation pressure of the solute, $\hat{\phi}_m$ is the supercritical fluid-phase fugacity coefficient of the solute, V_{sol} is the molar volume of the pure solute. The temperature dependence of the sublimation pressures of the solutes in question are given by Jones[17]. Molar volumes

of solid solutes of interest are found in International Critical Tables[18] as 110.6, 173.9, 96.5 mole/cm^3 for naphthalene, phenanthrene and benzoic acid reprectively. The values of fugacity coefficient of the solutes ($\hat{\phi}_m$) are obtained from the RP EOS[15] as described above.

The binary interaction coefficients δ_{ij} and δ_{ji} for naphthalene-, phenanthrene-, and benzoic acid-carbon dioxide systems are obtained through regression using Equation 12 and solubility data given in literature (Table 2).

The fugacity coefficient, $\hat{\phi}_m^{\infty}$, was calculated for infinite-dilution conditions (mole fraction of the solute in the mobile phase, $y_m = 10^{-8}$) using PRXEOS. It was seen that the value of $(\partial\hat{\phi}_m^{\infty}/\partial P)_{y_m}$ did not change significantly when the value of y_m was decreased below 10^{-6}. Due to the lack of solubility data for the CO_2-methoxy naphthalene system, binary interaction coefficients were taken to be equal to zero in order to estimate $\bar{V}_s^{\infty}$ and theoretical values of k.

Discussion of Results

The experimental data obtained in this study, when represented as a $\ln(ky_m\rho_m)$ versus P plot (Figure 2), is instrumental in validation of the thermodynamic model elaborated in the previous section. Although

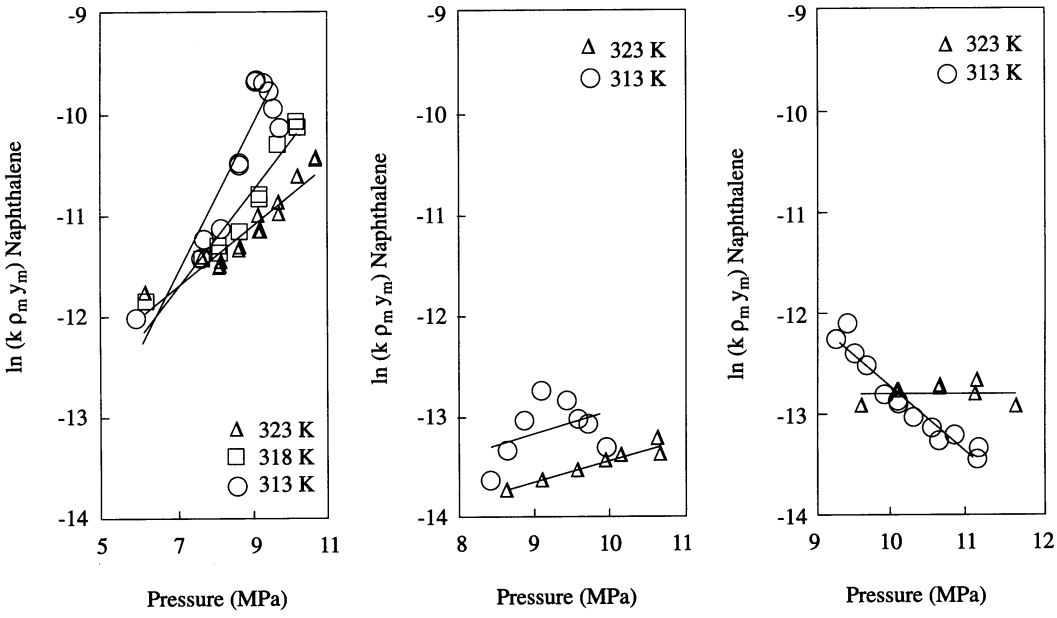

Figure 2. ln $(k\rho_m y_m)$ versus P for different solutes.

$\ln(ky_m\rho_m)$, elements of which are computed using approach A, is linear with pressure for operating conditions away from the immediate vicinity of the critical region of the mobile phase (e.g. 323 K), close to the critical region (e.g. 313K) this relationship is not linear.

$\bar{V}_s^{\infty}$ is calculated from the slope of the integrated form of Equation 7 which is shown in Figure 2 and summarized in Table 3. The sign of $\bar{V}_s^{\infty}$ is related to the intermolecular interactions between the solute and the stationary phase. The nonlinear behavior seen at 313 K (Figure 2) shows that the interaction between the stationary phase and the solute varies with pressure.

Bartle et al.[4,5] assumed $l/(y_m\rho_m)$ is linear with respect to k. This is valid for cases where $\bar{V}_s^{\infty}$ is constant and equal to the molar volume of the solid solute. This is equivalent to constant $\ln(ky_m\rho_m)$ in Figure 2. When SFC retention data obtained by Bartle and co-workers[4,5] is used to plot $\ln(k\rho_m y_m)$ against

pressure (Figure 3a), data obtained at 308 K lie around a horizontal line, however minima and maxima are observed at pressures lower than 15 MPa. At 318 K, data cannot be represented as a straight line. Bartle et al.[4,5] suggest that the solute/stationary-phase interactions are independent of the mobile phase in their case, and the stationary phase did not swell. Therefore, we suggest that the deviation of the $\ln(k\rho_m y_m)$ versus pressure plot from a straight line indicates changes in the intermolecular interactions between the stationary phase and the solute as the pressure varies. Yonker et al.[7] have also obtained retention data at high pressures for which $\ln(k\rho_m y_m)$ versus pressure relationship is not linear (Figure 3b).

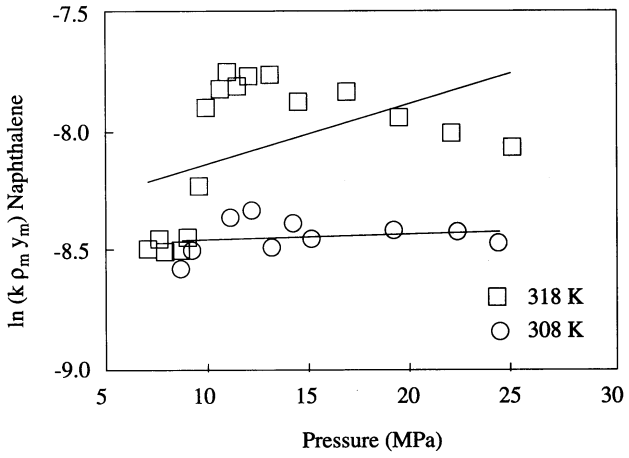

a) ln $(k\rho_m y_m)$ versus P for naphthalene calculated using data given in Reference 5.

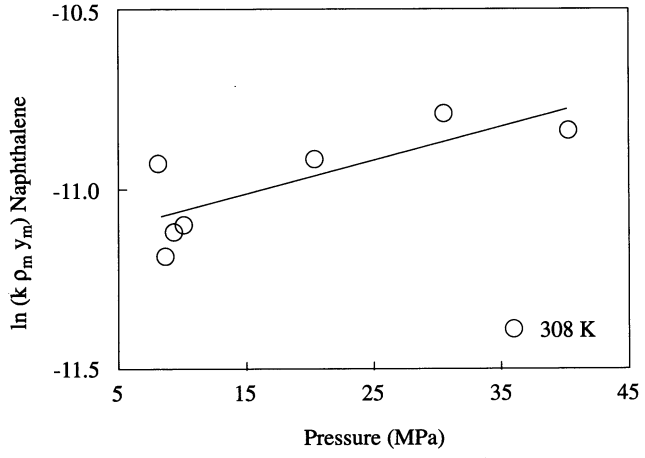

b) ln $(k\rho_m y_m)$ versus P for naphthalene calculated using data given in Reference 7.

Figure 3.

In order to compare approach A and approach B, $\bar{V}_m^{\infty}$ values for naphthalene, phenanthrene and benzoic acid are calculated using bulk solubility, through Equation 5 as well as infinite-dilution fugacity coefficients via Equation 9. Then, they are shown as a function of pressure for naphthalene (Figure 4a) and phenanthrene (Figure 4b). The $\bar{V}_m^{\infty}$ values calculated using different approaches are quite apart for naphthalene, especially near mobile phase critical point (Figure 4a). Due to the lower solubility of phenanthrene and benzoic acid in supercritical carbon dioxide, the differences between $\bar{V}_m^{\infty}$ values calculated using approaches A and B are small (Figure 4b). In approach B, plot of $\ln(k\rho_m/\hat{\phi}_m^{\infty}P)$ versus P should give a straight line according to Equation 10 (Figrue 5). Values of $\bar{V}_s^{\infty}$ are calculated from the slope of such plots (Table 3). Since the bulk solubility of naphthalene in carbon dioxide is about ten times higher than that of phenanthrene and benzoic acid, $\bar{V}_s^{\infty}$ values determined using bulk solubility and infinite dilution fugacity coefficients differ for naphthalene more than for the other two solutes (Table 3). For phenanthrene and benzoic acid, the theoretical predictions of lnk using $\bar{V}_s^{\infty}$ values calculated through both approaches are similar (Table 3).

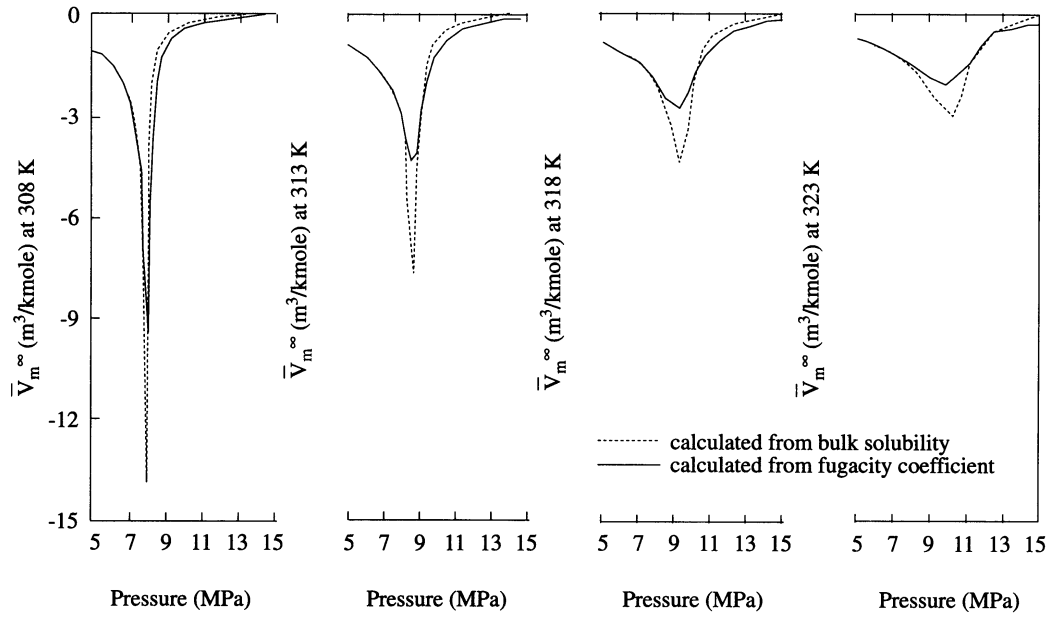

Figure 4a. $\bar{V}_m^\infty$ of naphthalene as a function of pressure

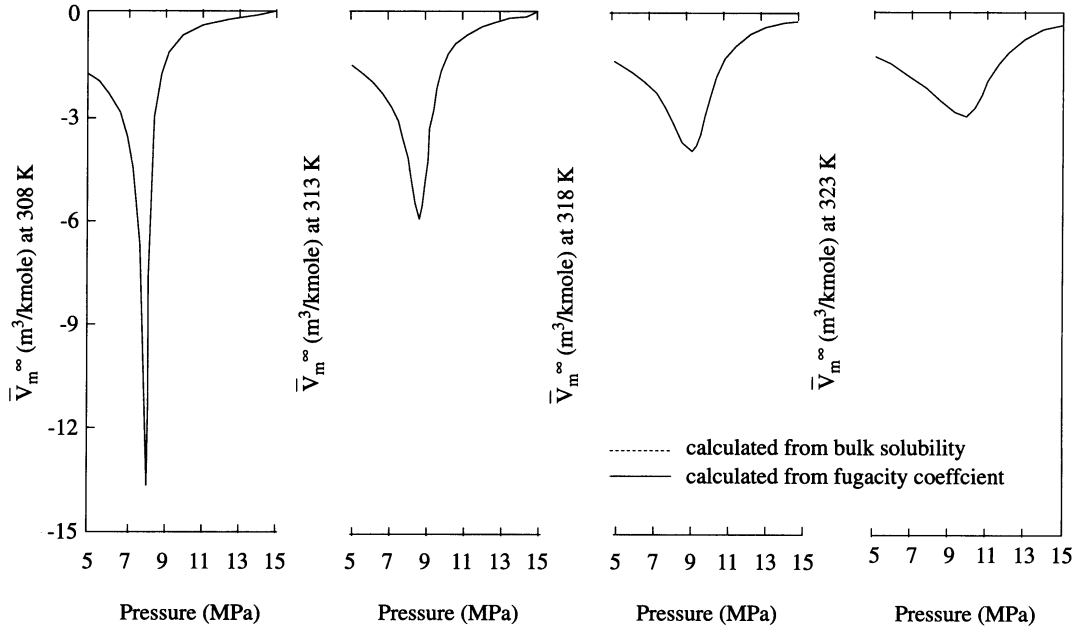

Figure 4b. $\bar{V}_m^\infty$ of phenanthrene as a function of pressure

Table 3. Infinite Dilution Partial Molar Volumes of Solutes in the Stationary Phase

		$\bar{V}_s^{\infty}$ [cm^3/gmol]		
Solute	**Approach**	**313 K**	**318 K**	**323 K**
Naphthalene	A	$-1801 \pm 26\%$	$-1174 \pm 22\%$	$-723 \pm 15\%$
Naphthalene	B	$-1166 \pm 22\%$	$-650 \pm 11\%$	$-422 \pm 18\%$
Phenanthrene	A	$1900 \pm 13\%$	n.e.	$164 \pm 202\%$
Phenanthrene	B	$2031 \pm 13\%$	n.e.	$133 \pm 250\%$
Benzoic Acid	A	$-449 \pm 255\%$	n.e.	$448 \pm 36\%$
Benzoic Acid	B	$-535 \pm 255\%$	n.e.	$-523 \pm 33\%$
2-Methoxy Naphthalene	B	$-1460 \pm 90\%$	n.e.	$-1036 \pm 20\%$

n.e.= no experiment

Values of $\bar{V}_s^{\infty}$ for 2-methoxy-naphthalene, for which no solubility data in carbon dioxide is available, were estimated using approach B (Table 3). Since the binary interaction coefficients could not be calculated in the absence of solubility data, they were assumed to be equal to zero. Although, it is theoretically possible to utilize approach A instead, the comparative sensitivity of approach B is far superior. This was shown for napthalene and phenanthrene for which the results are summarized in Table 4. This was further illustrated in Figure 6. The goodness of the fit of the experimental and theoretical k values at 323 K may be showing the negligible effect of the binary interaction coefficient in determining $\bar{V}_s^{\infty}$ of the solute at that temperature for the experimental pressure range.

Table 4. Effect of Interaction Coefficient on Infinite-Dilution Partial Molar Volumes of Solutes in the Stationary Phase for Approach A and B

		$\bar{V}_s^{\infty}[cm^3/gmol]$					
		APPROACH A			**APPROACH B**		
Solute	**Temperature** [K]	**Non Zero Interaction Coefficient**	**Zero Interaction Coefficient**	**% Deviation**	**Non Zero Interaction Coefficient**	**Zero Interaction Coefficient**	**% Deviation**
Naphthalene	313	-1801±26%	-5371±45%	198%	-1166±22%	-1605±18%	38%
Naphthalene	318	$-1174 \pm 17\%$	-5303±39%	352%	-650±11%	-951±8%	46%
Naphthalene	323	-723±15%	-3336±41%	361%	-422±18%	-661±11%	57%
Phenanthrene	313	1900± 13%	3793±11%	100%	2031±13%	1251±16%	38%
Pentanthrene	323	164±202%	-9369±57%	5778%	133±250%	-735±54%	653%

Figure 7 shows the dependence of solute retention on pressure and mobile-phase density as determined from the chromatographic experiments and from Equations 7 and 10 using values of $\bar{V}_s^{\infty}$ given in Table 3 for naphthalene at 313, 318, 323 K. The equilibrium solubility values are, in general, too high to be used as the mole fraction of naphthalene in the SFC at infinite dilution. Discrepancies are observed in plots drawn using different approaches; the second approach improved the fit of the k values to the experimental ones especially at low pressures. This may be due to the fact that $\bar{V}_m^{\infty}$ takes on very large negative values near the critical pressure (Figure 4a, 4b) and therefore $(\partial y_m/\partial P)_T$ term in Equation 6 is important. However, some general features are in common: At every temperature, the calculated values of lnk for naphthalene increase with increasing pressure after going through a minimum. Within the pressure range of the present study this minimum was not observed experimentally. The value of experimental k decreased monotonically for naphthalene at every temperature within the experimental pressure range.

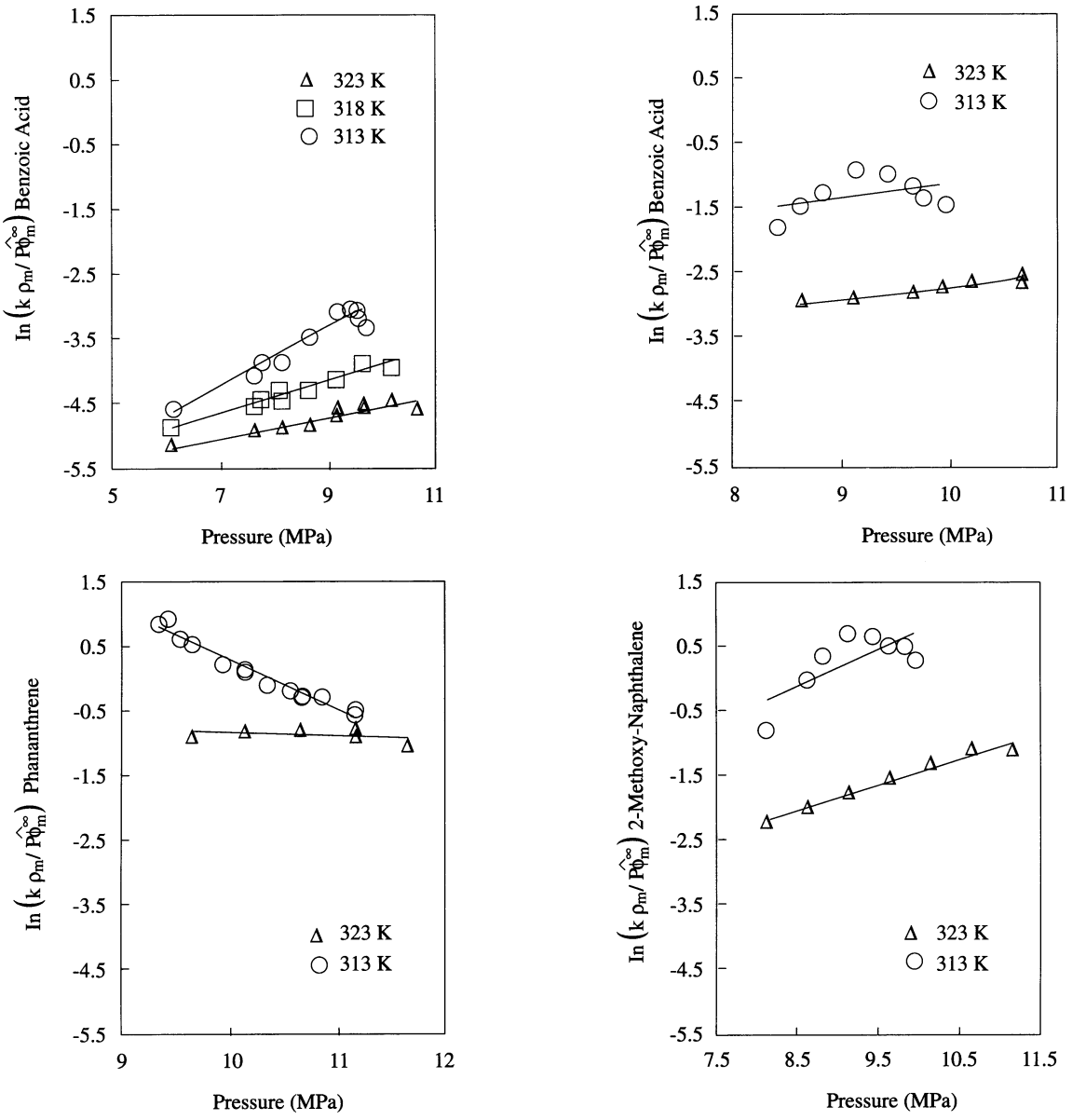

Figure 5. ln $(k\rho_m/\hat{\phi}^{\infty}_m P)$ versus P for different solutes.

Yonker and Smith[7] extended their experiments to higher pressures (on a different column) and did not observe any increase in the experimental k values with increasing pressure up to 40 MPa at 308 K for various solutes in carbon dioxide. This disagreement between the predicted increase and the experimental asymptotic decrease, as well as the discrepancies between the predicted and experimental retention values, may be indicating that the assumption of a constant $\bar{V}_s^{\infty}$ value is not correct. In such a case, one has to take into account the pressure dependence of $\bar{V}_s^{\infty}$ in the prediction of solute retention. Or else, swelling of the polymer in supercritical carbon dioxide may be significant. The value of the isothermal compressibility approaches zero at pressures higher than about 20 MPa. The solubility does not change much at pressures higher than 20 MPa either (Figure 9, b, c). An asymptotic approach to zero for lnk at high pressures suggests that the left hand side of Equation 6 also approximately equals zero. Therefore, $\bar{V}_s^{\infty}$ must be equal to V_{sol} at high pressures. This is confirmed by the high pressure retention data of Bartle and co-workers[4,5], Yonker and co-workers[7]. If $\ln(k\rho_m/\hat{\phi}^{\infty}_m P)$ versus pressure is plotted for the whole pressure range up to 400 bars, a constant slope is observed at pressures higher than 15 MPa (Figure 8). The slope is approximately equal to

$-V_{sol}/RT$ (Equation 10). Deviations from the straight line (minima and maxima) at pressures lower than 15 MPa may be showing that the variation in $\bar{V}_s^{\infty}$ with pressure is more significant near the critical region.

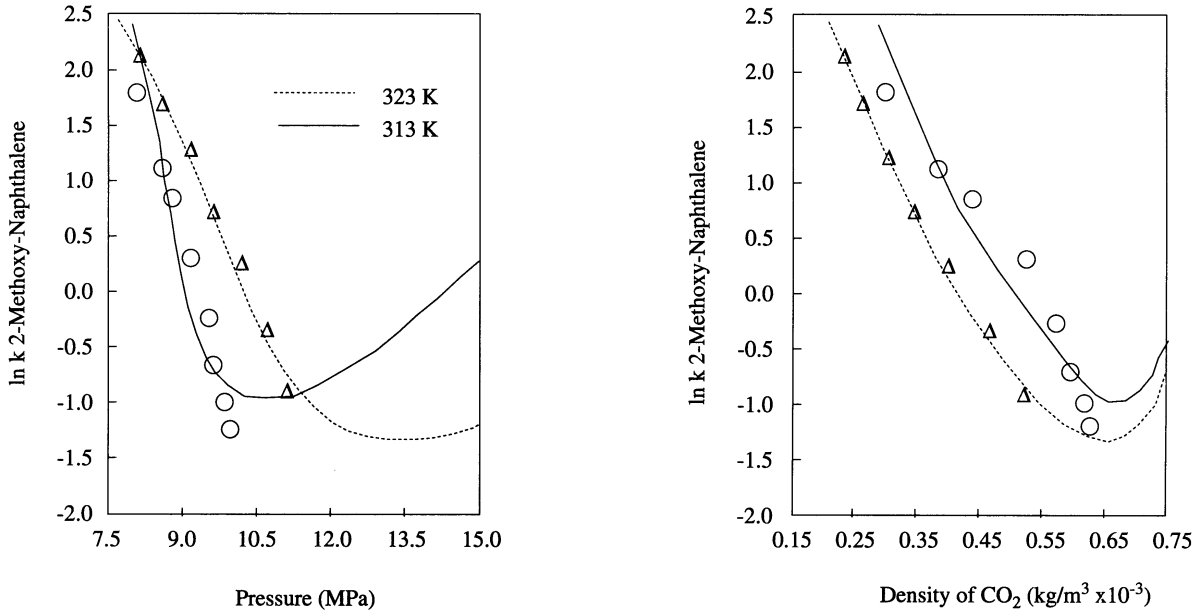

Figure 6. Retention of 2-methoxy-naphthalene as a function of pressure (Retention calculated using Approach B).

The disagreement between the predicted lnk values and the experimental values in the present case (Figure 7) may be attributed to the variation $\bar{V}_s^{\infty}$ with pressure, which was not included in the thermodynamic model, as well as to the swelling effect. Recent studies show that supercritical carbon dioxide causes significant degree of swelling of polymeric stationary-phase materials at elevated pressures[19,20]. Roth[21] calculated retention of naphthalene on polydimethyl-siloxane with carbon dioxide being the carrier fluid and concluded that the contribution of the swelling at 308 K and 7.46 MPa was $\sim$ 8% compared to the $[\bar{V}_m^{\infty} - \bar{V}_s^{\infty}]/RT$ and κ_m terms. The thermodynamic model used by Yonker and Smith[7] does not include the swelling term. In their case, they used crosslinked, 5% poly-methyl-phenyl-siloxane as the stationary phase. Methyl-siloxanes are known to be less compressible and less rubbery than dimethyl-siloxanes and there must also be some glassiness introduced because of the high degree of crosslinking. Therefore, the swelling term in our case may be more important than it is in the case of reference 7. The term which represents the swelling effect may be different at different temperatures and pressures and including this effect in the model might correct the prediction.

Figures 9a to 9c show the solubilities and retention of the three solutes of concern (naphthalene, phenanthrene and benzoic acid) as a function of pressure. The figures show a direct qualitative relation between the solubility and experimental retention values in terms of temperature. The effect of temperature on solubility of naphthalene in carbon dioxide can be discussed for three different pressure regions (Figure 9a). In the low-pressure region (less than the critical pressure of the mobile phase), the solubility of naphthalene in carbon dioxide increases as temperature increases. There is a cross-over region between the critical pressure of the mobile phase and approximately 10 MPa. In this region, the solubility increases with decreasing temperature for a given pressure. At pressures higher than approximately 10 MPa, the temperature dependence of the solubility at a fixed pressure is the same as in the first region (pressures less than the critical pressure of the mobile phase). This temperature effect in solubility is reflected on the

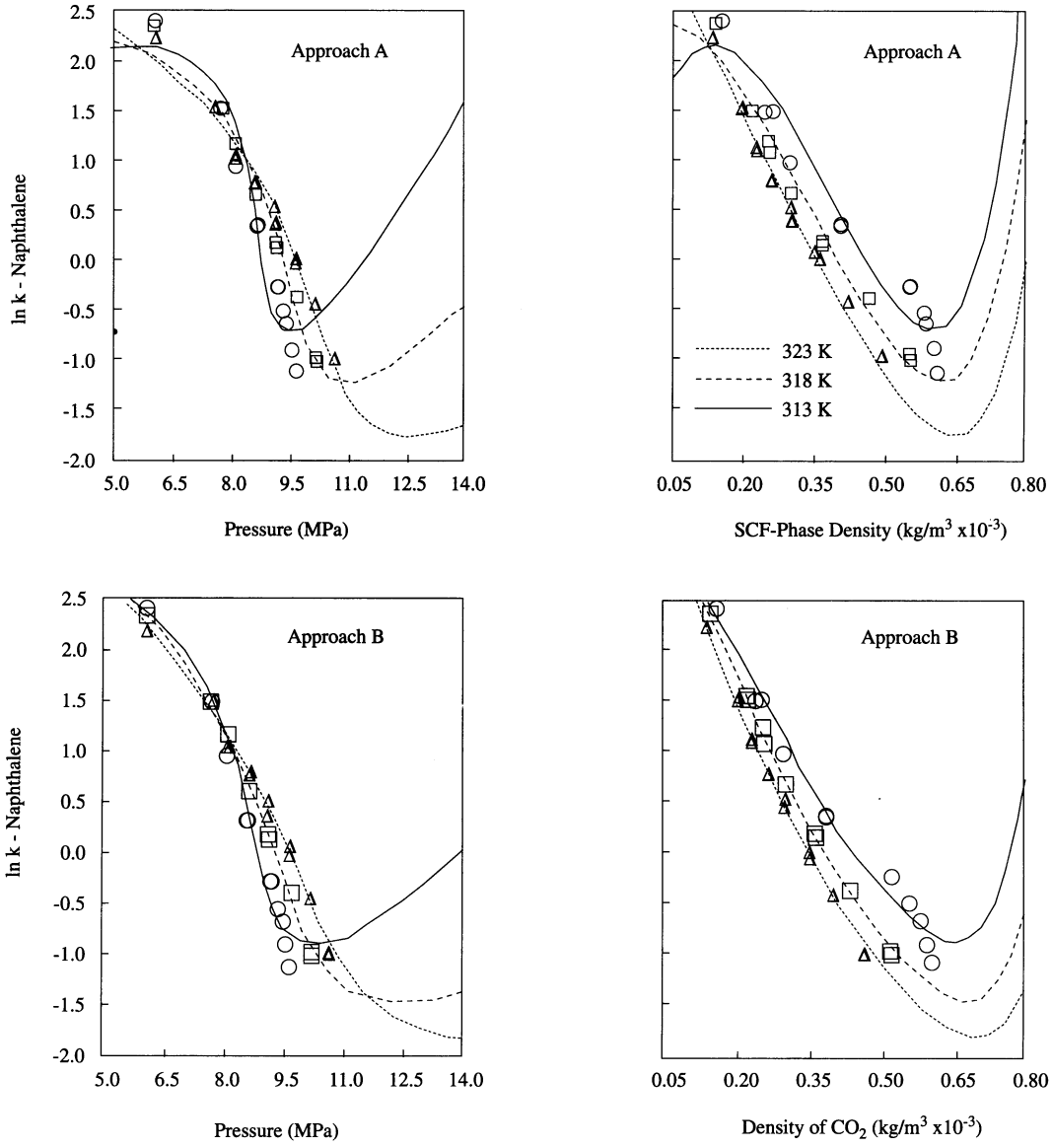

Figure 7. Comparison of approaches A and B for prediction of retention of naphthalene.

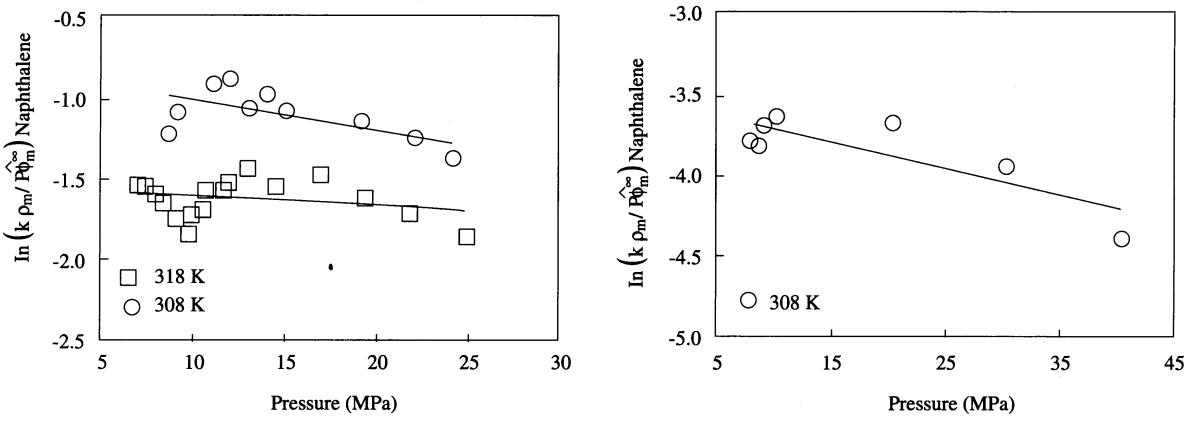

a) In $(k\rho_m/\hat{\phi}_m^{\infty}P)$ versus P for naphthalene calculated using data given in Reference 5.

b) In $(k\rho_m/\hat{\phi}_m^{\infty}P)$ versus P for naphthalene calculated using data given in Reference 7.

Figure 8.

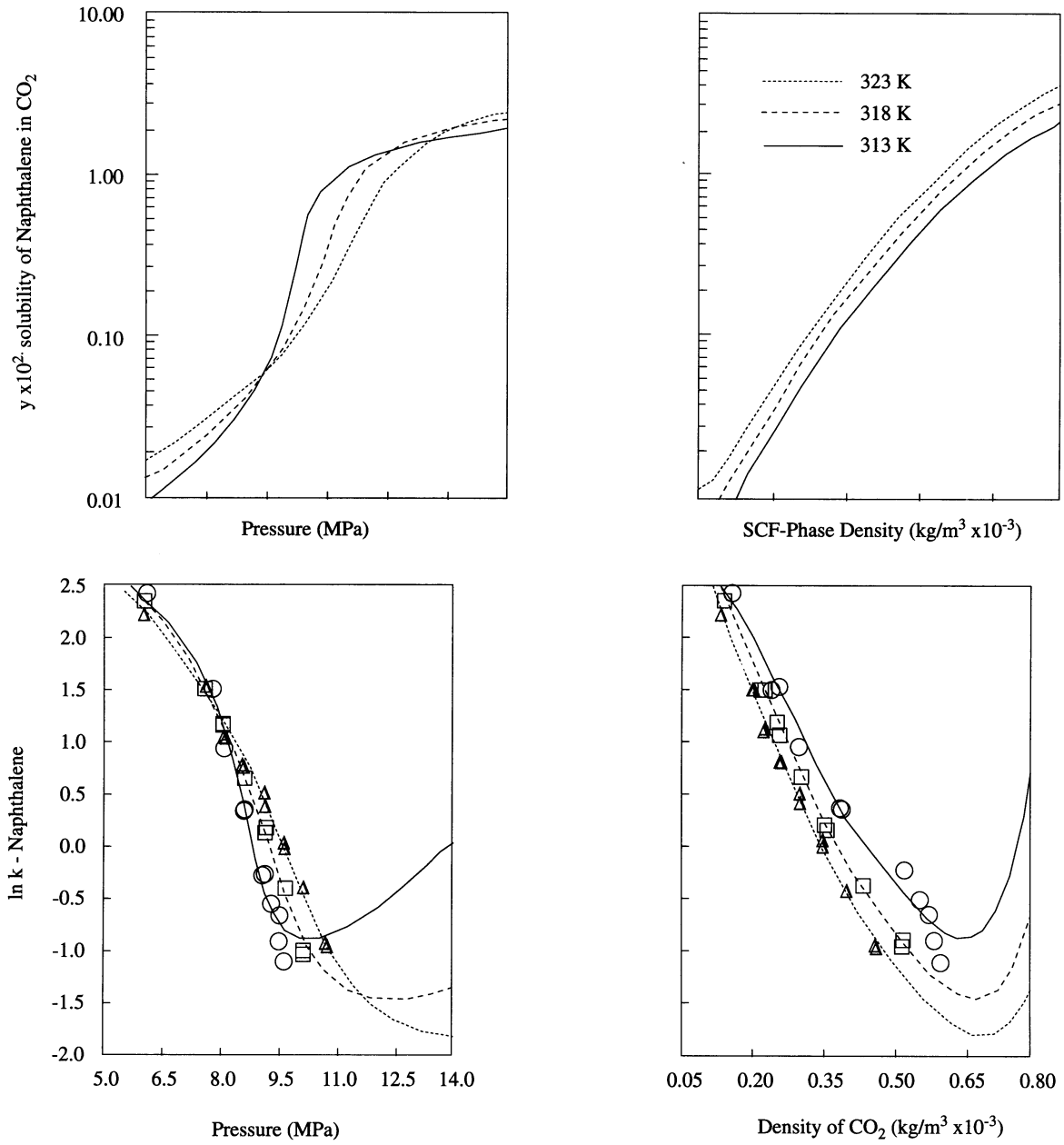

Figure 9a. Solubility and retention of naphthalene as a function of pressure and CO_2 density (Retention calculated using Approach B)..

solute retention (Figure 9a). At pressures less than the critical pressure of the mobile phase, solute retention decreases as the temperature increases; which is due to the increase in solubility of the solute in carbon dioxide. At pressure higher than the critical pressure of the mobile phase, the solute retention increases as temperature increases; which is a reflection of the effect of temperature on solute solubility in the solvent. When solubility of naphthalene in carbon dioxide is plotted as a function of the mobile phase density, the cross-over behavior is not observed (Figure 9a). At a given mobile phase density, solubility of naphthalene in carbon dioxide increases as temperature increases. Figure 9a also shows the effect of mobile phase density on the retention of naphthalene. At a given density, the increase in solubility with temperature is reflected on the density dependence of retention. As temperature increases, solubility increases and, as a result of this, the retention decreases (Figure 9a). This is valid over the entire range of density for the experimental data.

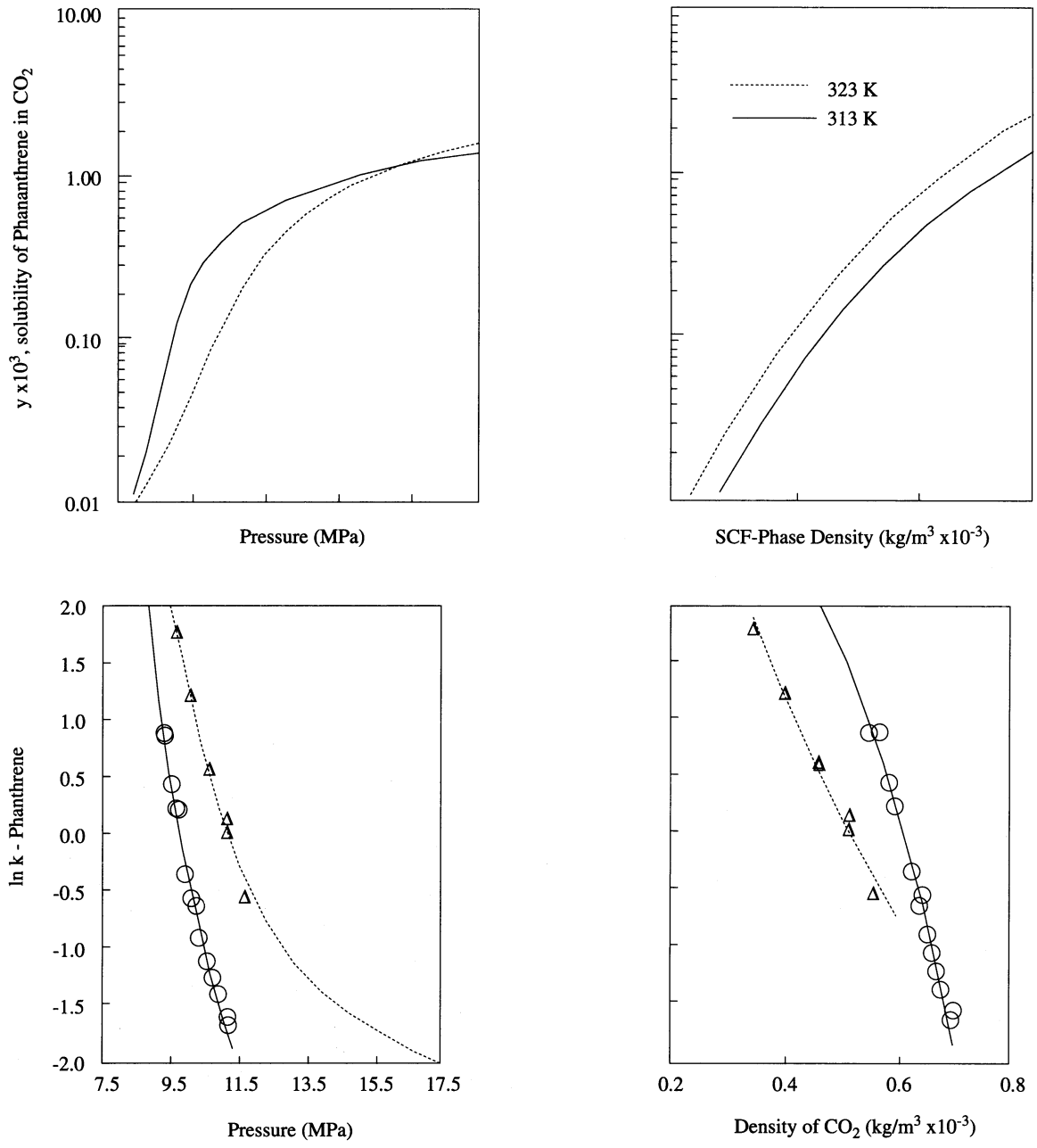

Figure 9b. Solubility and retention of phenanthrene as a function of pressure and CO_2 density (Retention calculated using Approach B)..

For other solutes, the experiments were performed only at pressures higher than the critical pressure of the mobile phase (Table 1). Within the experimental pressure range, the retention of the solutes increased (solubility of the solutes decreased) as temperature increased. Figure 9b shows the experimental and calculated retention of phenanthrene as a function of pressure at 313 and 323 K. The value of $\bar{V}_s^{\infty}$ for phenanthrene at 313 K is positive and much larger than the molar volume of the solid phenanthrene (Table 3). This large positive value of $\bar{V}_s^{\infty}$ results in a monotonic decrease in the value of lnk calculated from Equation 4 with pressure. The contribution of $\bar{V}_m^{\infty}$ terms in Equation 4 are negative. At 323 K, $\bar{V}_s^{\infty}$ for phenanthrene was found to be positive but slightly smaller than the molar volume of solid phenanthrene (Table 3). As a result of this, the predicted retention decreases with pressure, goes through a minimum at high pressure and then increases slowly. Values of $\bar{V}_s^{\infty}$ for benzoic acid at 313 and 323 K are both negative

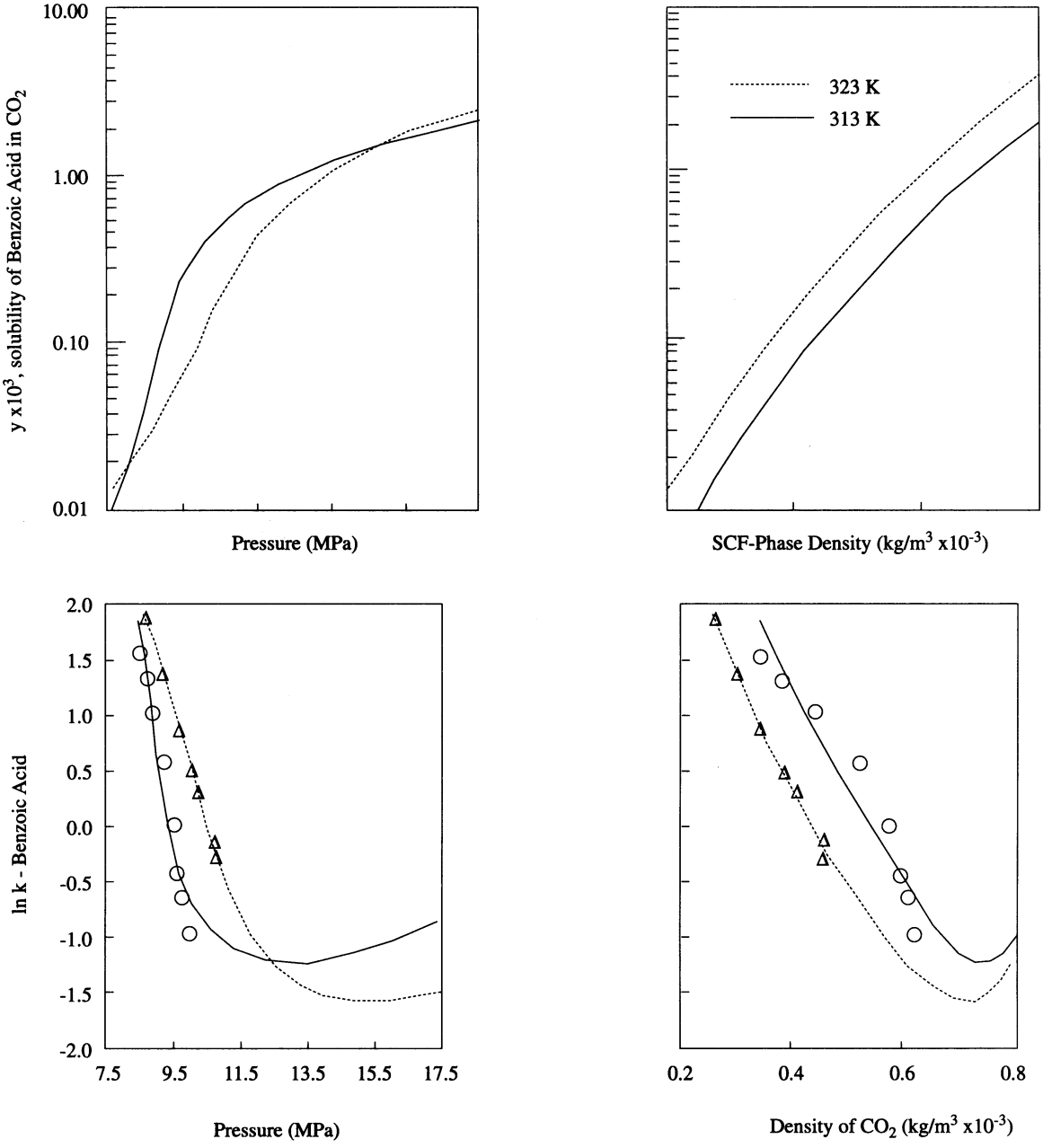

Figure 9c. Solubility and retention of benzoic acid as a function of pressure CO_2 density (Retention calculated using Approach B).

and close to each other (Table 3). Therefore, the predicted values of lnk show similar increase with pressure at both temperatures (Figure 9c). The calculated lnk values are closer to the experimental ones at 323 K than they are at 313 K.

Conclusion

The use of infinite-dilution fugacity coefficient instead of bulk solubility data in determining the partial molar volume of the solute in the mobile phase improves the prediction of the retention values of the solutes especially around the critical pressure and for solutes with appreciable bulk solubility in the mobile phase. However, the probably more significant contribution of the approach is in providing the means of estimating

$\bar{V}_s^{\infty}$ in the absence of solubility data.

Models which neglect the interaction of stationary phase and the mobile phase do not represent the experimental retention of solutes very well. This is particularly true in the vicinity of the critical point where $\bar{V}_s^{\infty}$ is shown to be pressure dependent.

In estimating thermophysical properties such as solubility, one should either use adsorption chromatography as opposed to partition or start with a model that does not neglect stationary phase/mobile-phase interactions.

These conclusion are further supported by analysis of new data extends the range of data available in literature. The data provided for 2-methoxy-naphthalene validates the utility of the proposed approach in instances where there is no solubility data.

LIST OF SYMBOLS

a_i, a_j	pure component parameter
a_{mix}	mixture parameter
c_m	concentration of the solute in the mobile phase
c_s	concentration of the solute in the stationary phase
k	capacity ratio
P	pressure
P_{sub}	sublimation pressure of the solute
R	universal gas constant
t	retention time of the solute
t_o	retention time of the nonsorbed (inert) compound
T	temperature
V_{sol}	molar volume of the solid solute
V_m	molar volume of the mobile phase
V_s	molar volume of the stationary phase
V_{tm}	total volume of the mobile phase
V_{ts}	total volume of the stationary phase
$\bar{V}_m^{\infty}$	infinite-dilution partial molar volume of the solute in the mobile phase
$\bar{V}_s^{\infty}$	infinite-dilution partial molar volume of the solute in the stationary phase
y_m	mole fraction of the solute in the mobile phase
y_s	mole fraction of the solute in the stationary phase

Greek Symbols:

δ_{ij}, δ_{ji}	binary interaction parameters
κ_m	isothermal compressibility of the mobile phase
ρ_m	molar density of the mobile phase
ρ_s	molar density of the stationary phase
$\hat{\phi}_m^{\infty}$	infinite-dilution fugacity coefficient of the solute in the mobile phase

References

1. U. Van Wasen, I. Swaid, G.M. Schneider, **Angew. Chem. Int. Ed. Engl. 19,** 575, (1980).
2. C.R. Yonker, B.W. Wright, S.L. Frye, R.D. Smith, **Supercritical Fluids** (Ed. T.G. Squires and M.E. Paulatis), American Chemical Society, Washington DC, 1987; Chapter 14.

3. M. Gitterman, I. Proccacia, **J. Chem. Phys., 78**, 2648, (1983).
4. K.D. Bartle, A.A. Clifford, S.A. Jafar, J.P. Kithinji, G.F. Shilstone, **J. Chromatogr. 517**, 459, (1990).
5. K.D. Bartle, A.A. Clifford, S.A. Jafar, **J. Chem. Soc. Faraday Trans., 86(5),** 855, (1990).
6. C.R. Yonker, R.D. Smith *Int. Symp. on Supercritical Fluids Proceedings*, **1988**, 439.
7. C.R. Yonker, R.D. Smith, **J. Phys. Chem., 92, 1664, (1988).**
8. C.R. Yonker, R.D. Smith, **J. Chromatogr., 459**, 183, (1988).
9. Z.S. Gonenc, A.K. Sunol, **Doga Tr. J. of Chemistry, 16**, 151, (1992).
10. J.M. Prausnitz, Molecular Thermodynamics of Fluid-Phase Equilibria, 2nd ed.; Prentice-Hall: New York, 1986.
11. M. McHugh, M.E. Paulatis, **J. Chem. Eng. Data, 25**, 326, (1980).
12. J.M. Dobbs, J.M. Wong, K.P. Johnston, K.P., **J. Chem. Eng. Data, 31**, 303, (1986).
13. R.T. Kurnik, S.J. Holla, R.C. Reid, **J. Chem. Eng. Data, 26**, 47, (1981).
14. J.M. Dobbs, J.M. Wong, R.LJ. Lahiere, K.P Johnston, **Ind. Eng. Chem. Res., 26,** 56, (1986).
15. D.Y. Peng, D.B. Robinson, **Ind. Eng. Chem. Fundam., 15**, 59, (1976).
16. A.Z. Panagiotopoulos, R.C. Reid, **ACS Symp. Ser.**, No. 30; American Chemical Societies: Washington D.mC., 1986, 371.
17. A.H. Jones, **Chem. Eng. Data, 5,** 196, (1960).
18. International Critical Tables, McGraw-Hill, N.Y, 1926-1930.
19. J. Shimm, K.P. Johnston, **AIChE J., 354(7),** 1097 (1989).
20. J. Shimm, K.P. Johnston, **J. Phys. Chem., 95,** 353 (1991).
21. M. Roth, **J. Phys. Chem. 94**, 4309, (1990).